Bioorg. Med. Chem. 28 (2020) 115793

Contents lists available at ScienceDirect

Bioorganic & Medicinal Chemistry

journal homepage: www.elsevier.com/locate/bmc

Divinylsulfonamides enable the construction of homogeneous antibody–drug conjugates

Rong Huang [a,b,1], Yao Sheng [a,1], Ding Wei [a,b,c], Wenwen Lu [a,b], Zili Xu [a,b], Hongli Chen [a,*], Biao Jiang [a,*]

[a] Shanghai Institute for Advanced Immunochemical Studies, ShanghaiTech University, 393 Middle Huaxia Road, Pudong, Shanghai 201210, China
[b] University of Chinese Academy of Sciences, 19A Yuquan Road, Shijingshan District, Beijing 100049, China
[c] Shanghai Advanced Research Institute, Chinese Academy of Sciences, Shanghai 201210, China

ARTICLE INFO

Keywords:
Divinylsulfonamides
Antibody-drug conjugates
Selectivity

ABSTRACT

Methods that site-specifically attach payloads to an antibody with controlled DAR (Drug-Antibody Ratio) are highly desirable for the generation of homogeneous antibody-drug conjugates (ADCs). We describe the use of *N*-phenyl-divinylsulfonamide scaffold as a linker platform to site-specifically construct homogeneous DAR four ADCs through a disulfide re-bridging approach. Several monomethyl auristatin E (MMAE)-linkers were synthesized and the drug-linkers that contain electron-donating groups on the phenyl of the linker showed high stability. Her2-targeted MMAE-linker-herceptin and EGFR targeted MMAE-linker-cetuximab conjugates were prepared. The conjugates demonstrated high efficacy and selectivity for killing target-positive cancer cells *in vitro*. The EGFR-targeted conjugates also showed significant antitumor activities *in vivo*.

1. Introduction

Antibody–drug conjugates (ADCs) combine the targeting ability of antibodies with the efficacy of the therapeutic payloads, demonstrating considerable promise for more targeted and precise therapeutics.[1–2] While the concept of ADCs is relatively straightforward, the development of functional and effective ADCs is remarkably challenging. In the past several years, a growing number of discontinuations of pre-clinical and clinical ADCs slows the development of ADCs.[3] However, the failures and setbacks did not limit the development of biotechnology and chemical conjugation methods for ADCs. With the approval of three ADCs (Polivy, Padcev and Enhertu) in 2019, Trodelvy and Blenrep in 2020, there are currently nine ADCs have received approval by the FDA. ADCs are worth more attention to reach their true potential.[4]

Linker technology and conjugation approach can strongly influence the drug-antibody ratio (DAR), pharmacokinetics, safety and also the ADC efficacy.[5] Chemical methods that site-specifically attach payloads to an antibody with controlled DAR are highly desirable for the generation of homogeneous ADCs.[6–7] Recently, reduction re-bridging strategy has emerged as a promising chemical approach: the four interchain disulfide bonds in IgG1 can be reduced and the resulting cysteine residues can be re-connected by a chemical linker, which allows the insertion of one drug per disulfide bond and thus DAR 4 ADCs can be achieved.[8] Many efforts have been made to develop chemical linkers for disulfide re-bridging. Bissulfone reagents represent the earliest developed linkers to re-connect disulfide bonds.[9–11] Then substituted maleimides and pyridazinediones have been developed to generate homogeneous ADCs using the reduction re-bridging strategy.[12–14] Later, alternatively new chemical entities have also been reported, such as dichloro- or dibromo-reagents,[15–17] thiol-yne coupling linkers,[18] divinylpyrimidine[19] and 3-bromo-5-methylene pyrrolones.[20]

Recently, we have developed divinylsulfonamides as specific linkers in the field of disulfide bonds stapling for peptides (Fig. 1**A**).[21] And we have also reported the use of bis(vinylsulfonyl)piperazines as efficient linkers to achieving controlled DAR two ADCs (Fig. 1**B**).[22] Whereas a drug loading of four has been demonstrated to significantly increase the therapeutic index for MMAE-based ADCs,[11,23] in this study, we describe an investigation in the development and application of divinylsulfonamides for the preparation of MMAE-based DAR 4 ADCs (Fig. 1**C**).

* Corresponding authors.
E-mail addresses: chenhl@shanghaitech.edu.cn (H. Chen), jiangbiao@shanghaitech.edu.cn (B. Jiang).
[1] These authors contributed equally to this work.

https://doi.org/10.1016/j.bmc.2020.115793
Received 31 July 2020; Received in revised form 23 September 2020; Accepted 24 September 2020
Available online 6 October 2020

2. Results and discussion

According to the previous study,[21] *N*-phenyl-divinylsulfonamide was employed as a scaffold with variant linkers attached to the phenyl for disulfide re-bridging. Three linker molecules that contained an alkyne as a handle to link a drug *via* click chemistry were designed and synthesized. As shown in scheme 1, *p*-aminophenol (**1**) was protected by Boc to give the product **2**, which was followed by the reaction with 3-bromoprop-1-yne to provide an alkyne derivative **3**. The Boc group was removed and the resulting product **4** was treated with 2-chloroethane-1-sulfonyl chloride (**5**) to obtain the ether linker **6**. Meanwhile, phenylamide and benzamide linkers **10** and **13** were also prepared. Commercially available *tert*-butyl (4-aminophenyl)carbamate (**7**) was reacted with hex-5-ynoic acid to afford compound **8**, followed by deprotection to give compound **9**. Finally, the phenylamide linker **10** was prepared by the reaction of **9** with the reagent **5** (Scheme 2). Benzamide linker (**13**) was synthesized from 4-aminobenzoic acid (**11**) which was reacted with prop-2-yn-1-amine, followed by the introduction of divinylsulfonamide under the same conditions as those used for the preparation of **6** and **10** (Scheme 3).

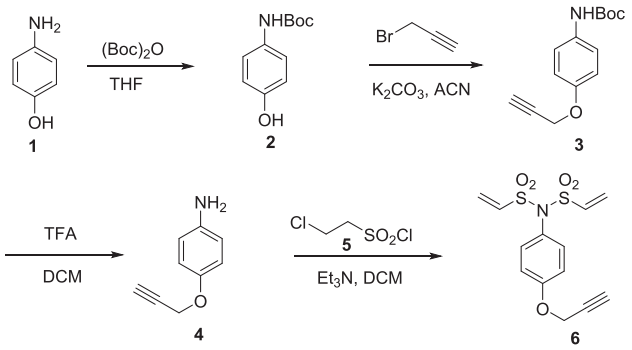

Scheme 1. Synthesis of Linker **6**.

On the other hand, the derivative of monomethyl auristatin E (MMAE), compound **14**, containing a PEG moiety and an azide tag, was prepared. The drug-linkers **15**–**17** were obtained by coupling compounds **6**, **10**, **13** with **14** using the Cu(I)-catalyzed azide–alkyne cycloaddition (CuAAC), respectively (Scheme 4).

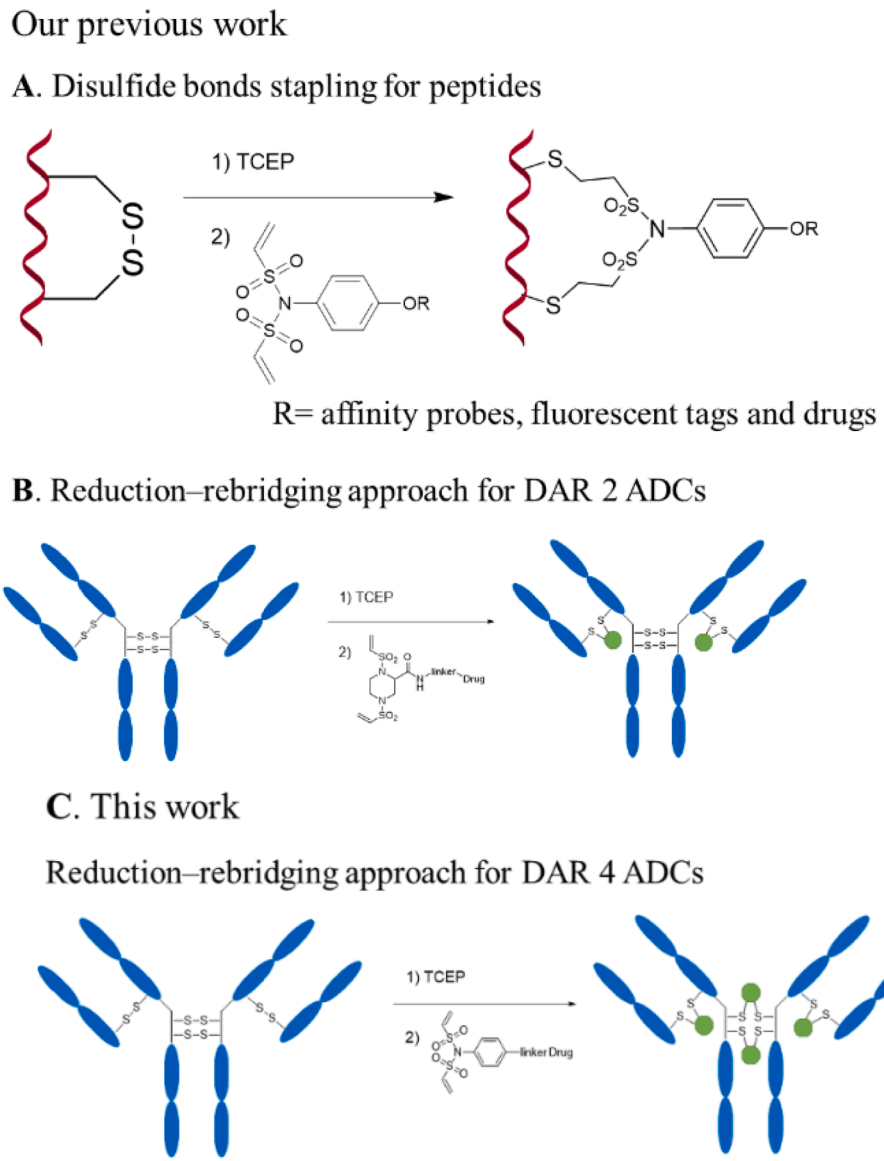

Fig. 1. (A) Previous work: disulfide bonds stapling for peptides; (B) Previous work: reduction–rebridging approach for DAR 2 ADCs; (C) This work: reduction rebridging approach for DAR 4 ADCs.

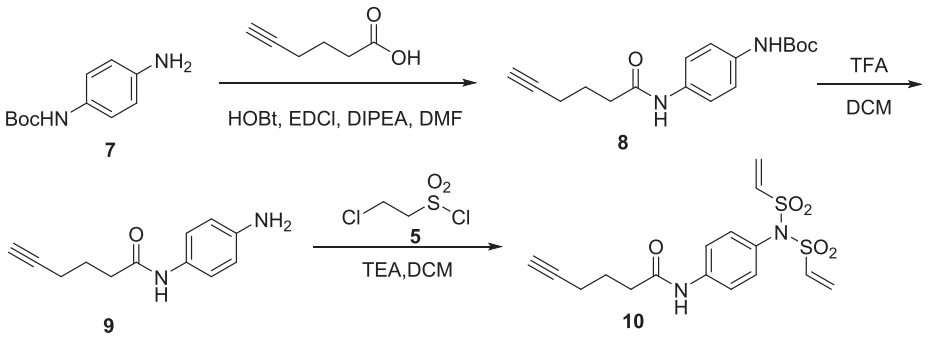

Scheme 2. Synthesis of Linker **10**.

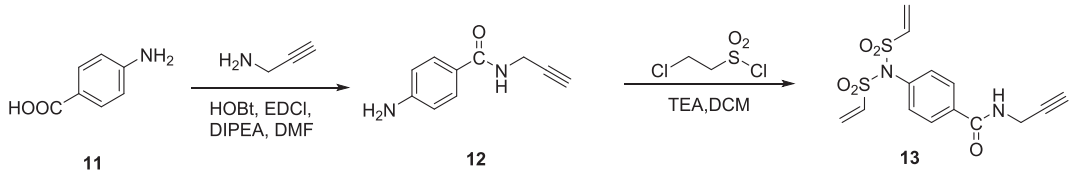

Scheme 3. Synthesis of Linker **13**.

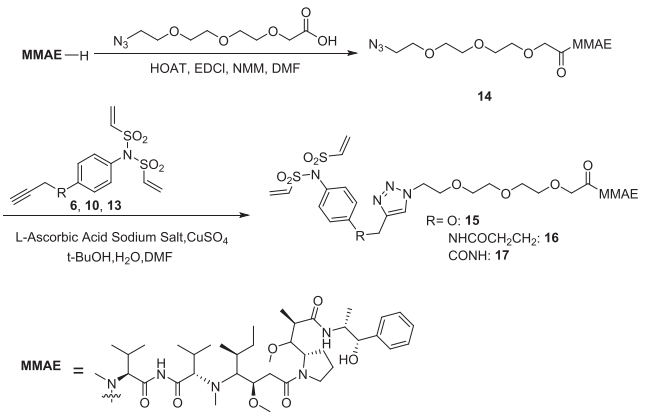

Scheme 4. Synthesis of drug-linkers **15**–**17**.

With the drug-linkers in hand, trastuzumab was employed for the preparation of ADCs. The antibody was reduced by treatment with tris (2-carboxyethyl)phosphine (TCEP) to release free thiols and the resulting mixture was subsequently incubated with the drug-linkers (**15**–**17**) (Fig. 2**A**). The mass spectrometry (MS) analysis showed that for the linkers **15** (MW = 1259.6, MW: molecular weight) and **16** (MW = 1314.7), the resulting ADCs **18** and **19** loaded four drug-linkers as the major species ($MW_{conjugate}$-$MW_{antibody} = 4*MW_{15\ or\ 16}$) and a few DAR two species were also observed (Fig. 2**B**). However, when the drug-linker **17** that contains the electron-withdrawing group on the phenyl of the linker reacted with the reduced antibody, it was tend to hydrolyze to yield the loss of one vinylsulfonamide product **17**–**1** (MW = 1196.7) and ethenesulfonic acid **17**–**2** (MW = 108.0). And **17-1** was attached to antibody to form the conjugated mixture **20** with average DAR 3.9 (Fig. 2**C**). We also found that the drug-linkers **15** and **16** retained high stability during long term storage (More than one year storage with HPLC purity:96% and 95%, respectively), while **17** presented a risk of instability and its HPLC purity was decreased to 80%, under the same storage conditions with those of **15** and **16** (**SI,** Fig. S1). The conjugates **18**–**20** were analyzed by SEC-HPLC and the result showed that the aggregation levels of all the ADCs were identical with the native antibody (Fig. 2**D**).

Then, the *in vitro* potencies of ADCs **18**–**20** were evaluated against HER2-positive (SK-BR-3) and HER2-negative (MDA-MB-468, HCC827 and MCF7) cancer cell lines. The FDA-approved HER2 targeted ADC trastuzumab emtansine (T-DM1), herceptin and MMAE were used as controls (Fig. 3**a-d**). All four cell lines are sensitive to free MMAE with high potencies. The ADCs **18**–**20** showed strong activities against the HER2-positive cancer cell (SK-BR-3) with IC_{50} values of 14.0 nM, 4.8 nM and 11.3 nM respectively, and their potencies were comparable with that of T-DM1 (6.4 nM). Whilst, the conjugates demonstrated significantly decreased activities in the antigen negative cell lines (>500 nM) (Fig. 3**e**). These results supported the ADCs' selectivity for killing HER2-positive cancer cells.

Cetuximab that binds to epidermal growth factor receptor (EGFR) was also used to the construction of EGFR-targeted ADCs. The conjugates **21**–**23** were obtained in a similar way with that of ADCs **18**–**20**. Likewise, the MS data showed that **21** and **22** were formed by disulfide re-bridging approach, whereas **23** was a heterogeneous mixture (Fig. S2). *In vitro* cytotoxicities of **21**–**23** were performed on HCC827 and NCI-H2228 cells (Fig. 4**a-b**). All the ADCs **21**–**23** showed strong activities on HCC827 cancer cells(EGFR-positive), with even lower IC_{50} values (0.5 ± 0.1 nM, 0.5 ± 0.1 nM, 0.8 ± 0.1 nM) than that of free MMAE (1.5 ± 0.2 nM). MMAE was also found to inhibit the proliferation of EGFR-negative cells(NCI-H2228) with IC_{50} value (2.2 ± 0.1 nM). When NCI-H2228 cells were incubated with ADCs **21**–**23**, no toxicity was observed in the study. (Fig. 4**c**).

The re-bridging conjugates **21** and **22** were further evaluated. Flow cytometry analysis was used to monitor affinity and internalization of the conjugates **21**, **22** and cetuximab. ADCs **21** and **22** were proven to have retained binding activities which were comparable to cetuximab in both EGFR-positive (HCC827, Fig. 5**a**) and EGFR-negative (NCI-H2228, Fig. 5**b**) cell lines. And the binding activities of all the molecules performed in a dose-dependent manner (Fig. 5**c**). In addition, internalization of the conjugates **21** and **22** in target cell was also comparable to cetuximab (Fig. 6).

The ability of the conjugates **21** and **22** to inhibit tumor growth *in vivo* was evaluated in a mouse xenograft study using HCC827 lung cancer cells derived tumors. Conjugates **21** and **22** groups received four doses of 20 mg/kg on days 0, 4, 8 and 12, injected intravenously. Tumor growth were inhibited significantly both by **21** and **22** treatments (Fig. 7**a**). Throughout the trial, the mice remained in good health and no weight loss or other overt toxicity (Fig. 7**b**). Our results showed that conjugates **21** and **22** are highly potent against $EGFR^+$ tumor *in vivo*.

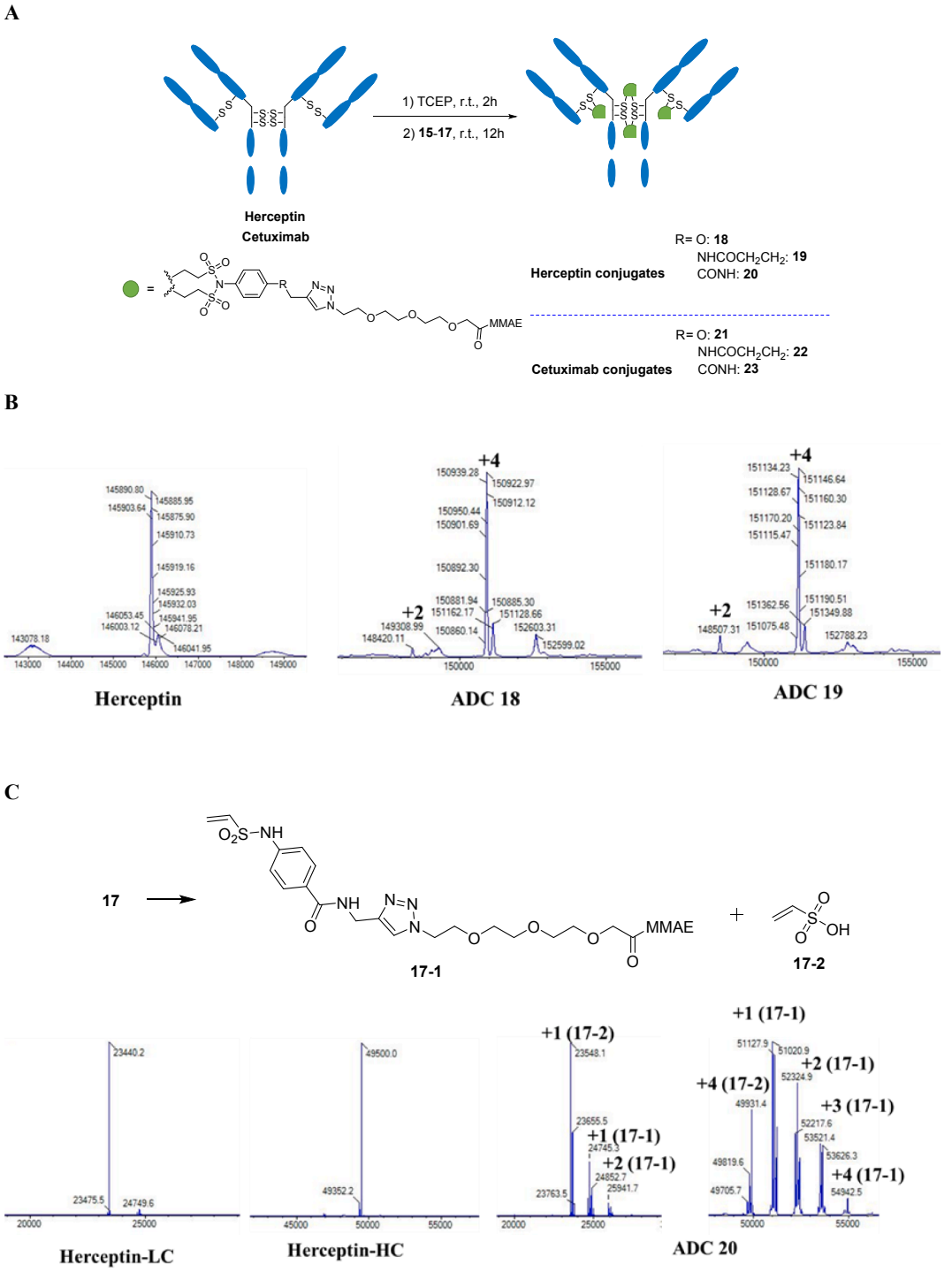

Fig. 2. Reaction of the drug-linkers **15**–**17** with herceptin or cetuximab and subsequent analysis. (A) Synthesis of herceptin-conjugated ADCs **18**–**20** and cetuximab-conjugated ADCs **21**–**23**. (B) MS analysis of ADCs **18**–**19**. (C) The scheme for the hydrolysis of the drug-linker **17** and MS analysis of heavy and light chain of herceptin and ADC **20**. (D) SEC analysis of herceptin and **18**–**20**.

3. Conclusions

In conclusion, *N*-phenyl-divinylsulfonamide linkages that contain electron-donating groups on the phenyl of the linker have shown the potencies to re-bridge the disulfide bonds to afford homogeneous DAR 4 ADCs. Linker-MMAE-ADCs demonstrated antigen-selective *in vitro* cytotoxicity. The conjugates also shown significant antitumor activities and were found to be well tolerated *in vivo*. We expect that this linker platform will facilitate its use for the development of ADCs candidates.

4. Experimental section

4.1. General experimental details

All chemical reagents and solvents were of analytical grade, obtained from commercial sources and used as supplied without further

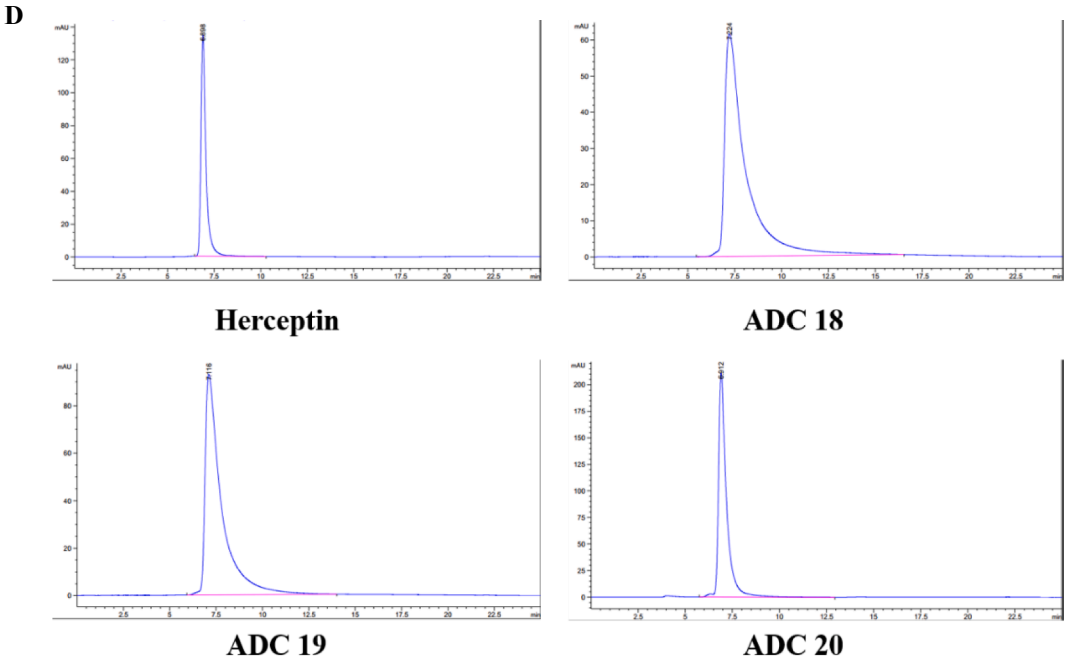

Fig. 2. (*continued*).

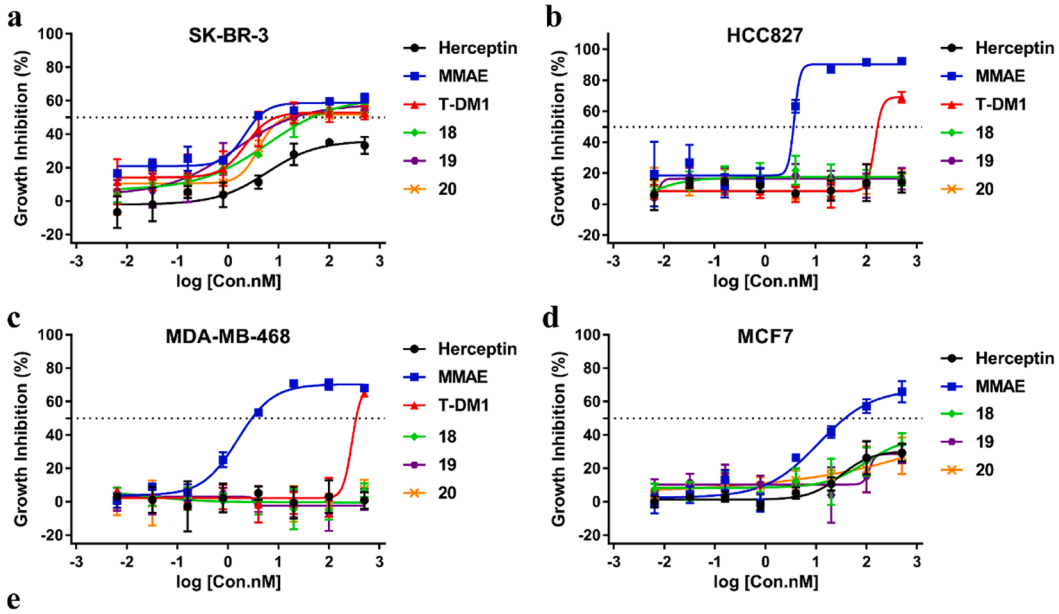

e

Cell lines	Herceptin	MMAE	T-DM1	**18**	**19**	**20**
SK-BR-3	222 ± 45.9	2.2± 0.4	6.4 ± 4.8	14.0 ± 5.9	4.8 ± 1.4	11.3 ± 2.7
HCC827	>500	2.7 ± 0.6	317 ± 93.7	>500	>500	>500
MCF7	>500	30.2 ± 4.3	——	487 ± 194	>500	>500
MDA-MB-468	>500	1.3 ± 0.2	220 ± 39.5	> 500	> 500	> 500

Fig. 3. *In vitro* potencies of ADCs **18**–**20**, MMAE, Herceptin and T-DM1. Potent activities in (a) HER2 positive cell line SK-BR-3, (b) HER2 negative cell line HCC827, (c) HER2 negative cell line MDA-MB-468, (d) HER2 negative cell line MCF7. (e) IC_{50} values (values = mean ± SD, n = 3) in both HER2 positive and negative cell lines.

purification unless indicated. trastuzumab and cetuximab were purchased from Shanghai huanyao biotechnology Co., Ltd. without further purification.

Non-aqueous reactions were conducted under a stream of dry nitrogen using oven dried glassware. Temperatures of 0 °C were maintained using an ice-water bath. Room temperature (rt) refers to ambient

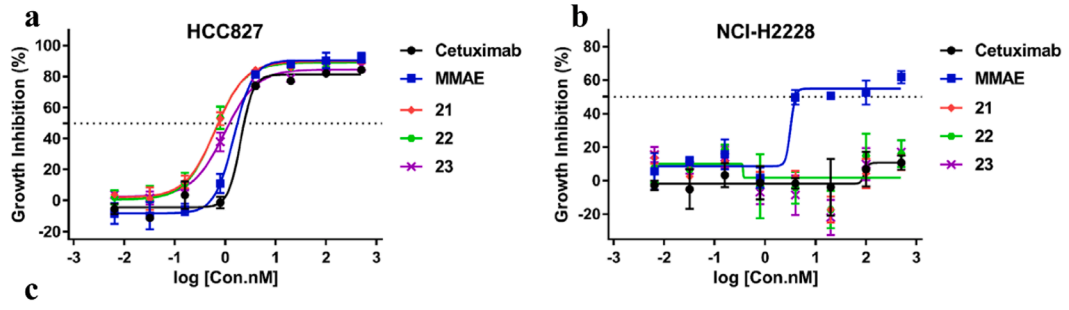

c

Cell lines	Cetuximab	MMAE	**21**	**22**	**23**
HCC827	2.0 ± 0.2	1.5 ± 0.2	0.5 ± 0.1	0.5 ±0.1	0.8 ± 0.1
NCI-H2228	>500	2.2 ± 0.5	>500	>500	>500

Fig. 4. *In vitro* potencies of ADCs **21**–**23**, MMAE and cetuximab. (a) Potent activities in EGFR positive cell line HCC827. (b) Potent activities in EGFR negative cell line NCI-H2228. (c) IC_{50} values (values = mean ± SD, n = 3) in both positive and negative cell lines.

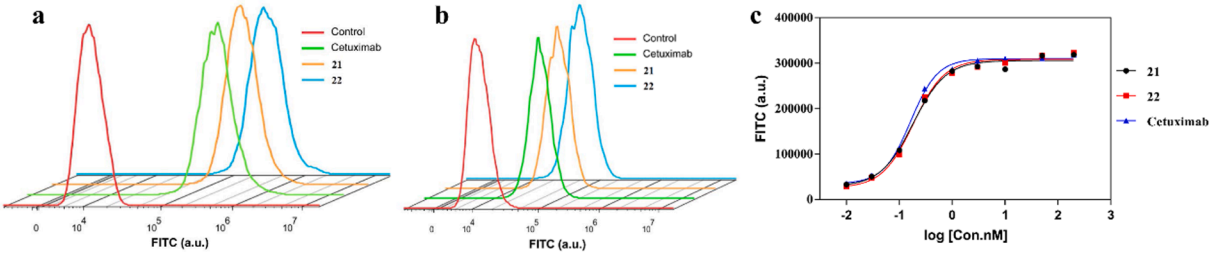

Fig. 5. Binding affinity of ADCs **21**, **22** and cetuximab as analyzed by flow cytometry. (a) in HCC827 cells. (b) in NCI-H2228 cells. (c) dose-dependent experiments.

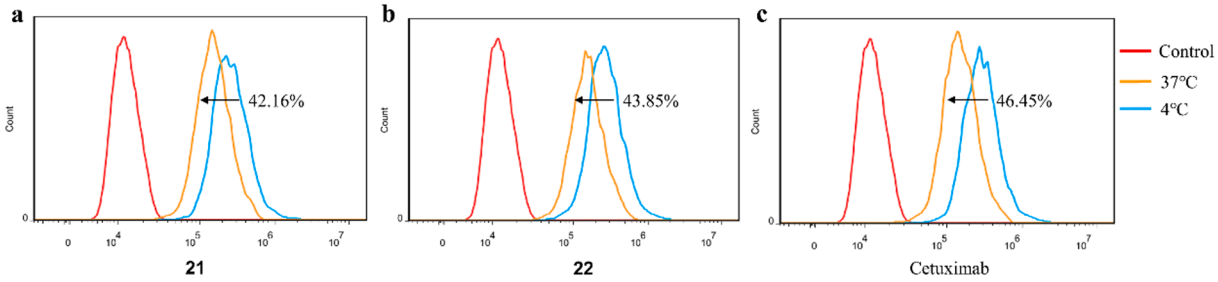

Fig. 6. Internalization of ADCs **21**, **22** and cetuximab in HCC827 cells as analyzed by flow cytometry. (a) **21**. (b) **22**. (c) Cetuximab.

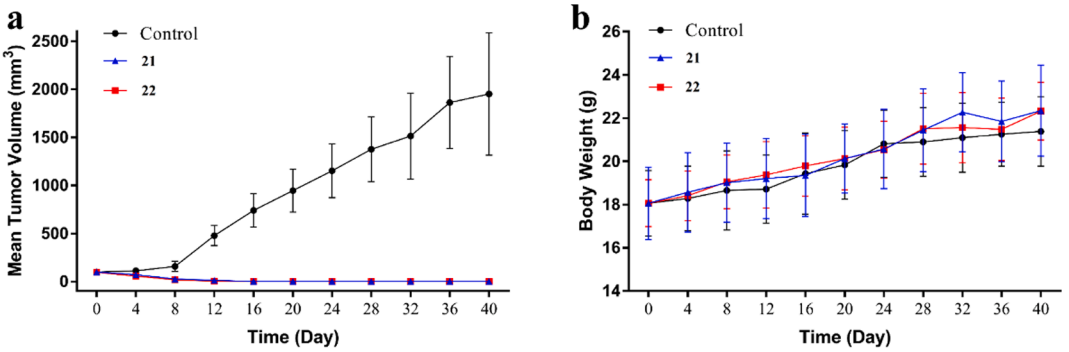

Fig. 7. *In vivo* efficacy of ADCs **21** and **22** against HCC827 subcutaneous tumor bearing models.

temperature. Yields refer to spectroscopically and chromatographically pure compounds unless otherwise stated. Reactions were monitored by thin layer chromatography (TLC) or liquid chromatography mass spectroscopy (LC-MS). TLC was purchased from Rushan Taiyang Desiccant Co., Ltd. and visualized by quenching of UV fluorescence (λ_{max} = 254 nm) or by staining with potassium permanganate. Flash chromatography was carried out on silica gel (200–300 mesh).

High-resolution mass spectra (HRMS-ESI) were obtained on an

ABsciex 4600 instrument. LC system: solvent A: 0.1% HCOOH on water; solvent B: acetonitrile; column: Agela Technologies C18 column (2.1 × 100 mm, 3 μm) at 30 °C; gradient: 0–3 min 5–100% B, 3–3.5 min 100% B, 3.51–5 min 5% B at flow rate of 0.4 mL/min; detector: UV detection (λ_{max} = 220–254 nm). ESI refers to the electrospray ionisation technique. Analytical high performance liquid chromatography (HPLC) was performed on SHIMADZU LC-30AD machine, using an Agela Technologies C18 column (2.1X100 mm, 3 μm). LC system: solvent A: 0.5% (v/v) TFA in H_2O; solvent B: acetonitrile at 30 °C; gradient: 0–10 min 10–100% B, 10–12 min 100% B at flow rate of 0.4 mL/min; detector: UV detection (λ_{max} = 220–254 nm). Proton and carbon nuclear magnetic resonance (NMR) were recorded using an internal deuterium lock on Bruker Avance 500 Cryo Ultrashield (500 MHz, 126 MHz). Tetramethylsilane was used as an internal standard. In proton NMR, chemical shifts (δ_H) are reported in parts per million (ppm), to the nearest 0.01 ppm and are referenced to the residual non-deuterated solvent peak ($CDCl_3$: 7.26, DMSO-d_6: 2.50, CD_3OD: 3.31, D_2O: 4.79). Coupling constants (*J*) are reported in Hertz (Hz) to the nearest 0.1 Hz. Data are reported as follows: chemical shift, multiplicity (s = singlet; d = doublet; t = triplet; q = quartet; qn = quintet; sep = septet; m = multiplet; or as a combination of these, e.g. dd, dt etc.), integration and coupling constant (s). In carbon NMR, chemical shifts (δ_C) are quoted in ppm, to the nearest 0.1 ppm, and are referenced to the residual non-deuterated solvent peak ($CDCl_3$: 77.16, DMSO-d_6, 39.52, CD_3OD: 49.00). The deuterated solvents employed were purchased from Energy Chemical. Spectra were analyzed with MestReNova.

Protein MS was performed on an ABsciex 4600 using a GL Sciences C4 column (2.1X150 mm, 5 μm). H_2O with 0.1% formic acid (solvent A) and acetonitrile (solvent B), were used as the mobile phase at a flow rate of 0.4 mL/min. The gradient was programmed as follows: 0–2.5 min 15% B, 2.5–5 min 15–95% B, 5–6.5 min 95% B, 6.51–8.0 min 5% B. The electrospray source was operated with a capillary voltage of 2.0 kV and a cone voltage of 40 V. Nitrogen was used as the desolvation gas at a total flow of 850 L/h. Total mass spectra were reconstructed from the ion series using the MaxEnt algorithm preinstalled on PeakView2.2 software (Version1.7.1 from AnalystTF) according to the manufacturer's instructions. Antibody samples were deglycosylated with Endo S prior to MS analysis. Size-exclusion chromatography (SEC) was performed using Agilent technologies 1260 Infinity. Mobile phase is Phosphate Buffered Saline (PBS (pH 7.4)). LC conditions: TSKgel G3000SWXL column: 7.8 × 300 mm, 5 μm, column temperature: 40 °C, λ = 280 nm, gradient: 0–20 min 100% PBS (pH 7.4), flow rate: 1 mL/min.

4.2. Chemical synthesis

4.2.1. Tert-butyl (4-hydroxyphenyl)carbamate (2)

A solution of 4-aminophenol (2.0 g, 18.3 mmol), di-*tert*-butyl dicarbonate (5.0 mL, 22 mmol) and triethylamine (5.0 mL, 36.6 mmol) in THF (50 mL) was stirred for overnight at room temperature. The mixture was concentrated under vacuum and the residue was purified by column chromatography to afford 3.27 g (15.6 mmol, 96%) yield of **2** as a white solid. ^{1}H NMR (500 MHz, DMSO-d_6) δ 9.04 (s, 1H), 8.99 (s, 1H), 7.22 (d, J = 7.1 Hz, 2H), 6.71–6.58 (m, 2H), 1.45 (s, 9H) ppm. ^{13}C NMR (126 MHz, DMSO-d_6) δ 153.06, 152.56, 131.08, 119.99, 115.07, 78.45, 28.24 ppm. ESI-HRMS calcd for $C_{11}H_{16}NO_3$ [(M + H)$^+$]: 210.1130, found:210.1154.

4.2.2. 4-(prop-2-yn-1-yloxy)aniline (4)

Tert-butyl (4-hydroxypHenyl)carbamate (**2**) (1.7 g, 8.1 mmol), 3-bromopropyne (0.84 mL, 9.7 mmol) and potassium carbonate (3.3 g, 24.3 mmol) were dissolved in DMF (30 mL). The reaction mixture was stirred at room temperature for overnight followed that water (600 mL) and ethyl acetate (3 × 50 mL) were added to extract the product. The combined organic extracts were washed sequentially with saturated $NaHCO_3$ (20 mL), NH_4Cl (20 mL) and brine (20 mL) and dried over anhydrous Na_2SO_4. The solvent was removed under vacuum and the residue was dissolved in DCM (30 mL). The solution was cooled to 0 °C with ice-bath followed trifluoroacetic acid (12 mL) added, and then the reaction mixture was stirred for 1 h under ice-bath. The mixture was concentrated under vacuum and residue was purified by column chromatography on a gradient form petroleum ether to 10% ethyl acetate/0.5% triethylamine in petroleum ether to afford 1.0 g (6.8 mmol, 84%) yield of **4** as red oil. ^{1}H NMR (500 MHz, $CDCl_3$) δ 6.80 (dd, J = 8.7, 1.6 Hz, 2H), 6.60 (dd, J = 8.8, 3.1 Hz, 2H), 4.58 (t, J = 2.4 Hz, 2H), 3.49 (s, 2H), 2.51 (d, J = 2.3 Hz, 1H) ppm. ^{13}C NMR (126 MHz, $CDCl_3$) δ 150.38, 140.99, 116.23, 116.09, 79.15, 75.27, 56.57 ppm. ESI-HRMS calcd for $C_9H_{10}NO$ [(M+H)$^+$]: 148.0762, found:148.0715.

4.2.3. N-(4-(prop-2-yn-1-yloxy)phenyl)-N-(vinylsulfonyl) ethenesulfonamide (6)

A stirred solution of 4-(prop-2-yn-1-yloxy)aniline (**4**) (180 mg, 1.22 mmol) and triethylamine (1.0 mL, 7.32 mmol) in DCM (15 mL) was cooled to 0 °C with ice-bath and 2-chloroethanesμlfonyl chloride (288 μL, 2.69 mmol) was then injected slowly. The reaction mixture was stirred at 0 °C for 20 min, and water (5 mL) was added. The product was extracted with DCM (3 × 15 mL). The combined organic extracts were washed with brine (10 mL) and dried over anhydrous Na_2SO_4. The solvent was removed under vacuum and residue was purified by column chromatography on a gradient form petroleum ether to 20% ethyl acetate in petroleum ether to afford 252 mg (0.77 mmol, 64%) yield of **6** as a slightly yellow solid. ^{1}H NMR (500 MHz, $CDCl_3$) δ 7.23–7.17 (m, 2H), 7.09–6.96 (m, 4H), 6.28 (d, J = 16.6 Hz, 2H), 6.14 (d, J = 9.9 Hz, 2H), 4.70 (d, J = 2.4 Hz, 2H), 2.56 (t, J = 2.4 Hz, 1H) ppm. ^{13}C NMR (126 MHz, $CDCl_3$) δ 159.16, 136.18, 132.24, 129.79, 126.81, 115.76, 77.97, 76.37, 56.17 ppm. ESI-HRMS calcd for $C_{13}H_{14}NO_5S_2$ [(M+H)$^+$]: 328.0313, found:328.0352.

4.2.4. Tert-butyl (4-(hex-5-ynamido)phenyl)carbamate (8)

Tert-butyl (4-aminophenyl)carbamate (2.291 g, 11 mmol), hex-5-ynoic acid (1.1213 g, 10 mmol), HOBt (1.633 g, 12 mmol), EDCl (2.30 g, 12.0 mmol) and N'*N*-diisopropylethylamine (4.958 mL, 30 mmol) were dissolved in DCM (30 mL). The reaction mixture was stirred at room temperature overnight followed that water (100 mL) and DCM (3 × 50 mL) were added to extract the product. The combined organic extracts were washed sequentially with saturated $NaHCO_3$ (20 mL), NH_4Cl (20 mL) and brine (20 mL) and dried over anhydrous Na_2SO_4. The solvent was removed under vacuum and residue was purified by column chromatography on a gradient form petroleum ether to 50% ethyl acetate in petroleum ether to afford 2.11 g (7 mmol, 70%) yield of **8** as a yellow solid. ^{1}H NMR (500 MHz, CD_3OD) δ 7.47–7.40 (m, 2H), 7.33 (d, J = 8.8 Hz, 2H), 2.50–2.44 (m, 2H), 2.28 (d, J = 2.6 Hz, 1H), 2.27–2.24 (m, 2H), 1.87 (p, J = 7.0 Hz, 2H), 1.51 (s, 9H). ^{13}C NMR (126 MHz, CD_3OD) δ 172.15, 153.99, 135.41, 133.37, 120.48, 118.81, 82.77, 79.39, 68.90, 35.15, 27.35, 24.38, 17.30. ESI-HRMS Calculated for $C_{17}H_{23}N_2O_3$ [M+H]$^+$:303.1709, Found:303.1720.

4.2.5. N-(4-aminophenyl)hex-5-ynamide (9)

Tert-butyl (4-(hex-5-ynamido)phenyl)carbamate (**8**) (2.11 g,7 mmol) was dissolved in DCM (20 mL). The solution was cooled to 0 °C with ice-bath followed by trifluoroacetic acid (4 mL) was added, and then the reaction mixture was stirred for 6 h under ice-bath. The mixture was concentrated under vacuum and the residue was purified by column chromatography on a gradient form petroleum ether to 30% ethyl acetate (0.5% triethylamine in petroleum ether) to afford 1.23 g (6.08 mmol, 87%) yield of **9** as yellow solid. ^{1}H NMR (500 MHz, CD_3OD) δ 7.28–7.22 (m, 2H), 6.72–6.63 (m, 2H), 2.48–2.38 (m, 2H), 2.29–2.20 (m, 3H), 1.91–1.81 (m, 2H). ^{13}C NMR (126 MHz, CD_3OD) δ 172.04, 144.16, 129.26, 121.99, 115.33, 83.00, 69.05, 35.15, 24.54, 17.40. ESI-HRMS Calculated for $C_{12}H_{15}N_2O$ [M+H]$^+$:203.1184, Found:203.1151.

4.2.6. N-(4-(N-(vinylsulfonyl)vinylsulfonamido)phenyl)hex-5-ynamide (10)

A stirred solution of *N*-(4-aminophenyl)hex-5-ynamide (**9**) (1.23 g, 6.08 mmol) and triethylamine (2.53 mL, 18.25 mmol) in DCM (20 mL) was cooled to 0 °C with ice-bath and 2-chloroethanesμlfonyl chloride (1.97 mL, 18.25 mmol) was then injected slowly. The reaction mixture was stirred at 0 °C for 1 h, and water (100 mL) was added. The product was extracted with DCM (3 × 20 mL). The combined organic extracts were washed with brine (10 mL) and dried over anhydrous Na_2SO_4. The solvent was removed under vacuum and residue was purified by column chromatography on a gradient form petroleum ether to 30% ethyl acetate in petroleum ether to afford 1.91 g (5 mmol, 82%) yield of **10** as a yellow solid. ^{1}H NMR (500 MHz, CD_3OD) δ 7.68–7.61 (m, 2H), 7.25–7.19 (m, 2H), 7.11 (dd, J = 16.3, 10.0 Hz, 2H), 6.25 (dd, J = 7.8, 0.6 Hz, 2H), 6.22 (d, J = 0.6 Hz, 2H), 2.53 (t, J = 7.5 Hz, 2H), 2.32–2.24 (m, 3H), 1.93–1.84 (m, 2H). ^{13}C NMR (126 MHz, CD_3OD) δ 172.54, 140.50, 136.23, 131.36, 129.25, 128.94, 119.89, 82.71, 68.93, 35.20, 24.11, 17.23. ESI-HRMS Calculated for $C_{16}H_{19}N_2O_5S_2$ $[M+H]^+$:383.0735, Found:383.0748.

4.2.7. 4-amino-N-(prop-2-yn-1-yl)benzamide (12)

4-aminobenzoic acid (1.50854 g, 11 mmol), propargylamine (0.686 mL, 10 mmol), HOBt (1.633 g, 12 mmol), EDCl (2.30 g, 12.0 mmol) and N'*N*-diisopropylethylamine (4.958 mL, 30 mmol) were dissolved in THF (30 mL). The reaction mixture was stirred at room temperature overnight. The mixture was concentrated under vacuum and the residue was dissolved with DCM (30 mL) and water (100 mL) and DCM (3 × 50 mL) were added to extract the product. The combined organic extracts were washed sequentially with saturated $NaHCO_3$ (20 mL), NH_4Cl (20 mL) and brine (20 mL) and dried over anhydrous Na_2SO_4. The solvent was removed under vacuum and residue was purified by column chromatography on a gradient form petroleum ether to 50% ethyl acetate in petroleum ether to afford 1 g (5.74 mmol, 57%) yield of **12** as a slightly yellow solid. ^{1}H NMR (500 MHz, DMSO-d_6) δ 8.42 (t, J = 5.1 Hz, 1H), 7.58 (d, J = 8.5 Hz, 2H), 6.54 (d, J = 8.5 Hz, 2H), 5.65 (s, 2H), 3.99 (dd, J = 5.4, 2.2 Hz, 2H), 3.04 (s, 1H). ^{13}C NMR (126 MHz, DMSO-d_6) δ 166.42, 152.31, 129.32, 120.93, 113.03, 82.45, 72.83, 28.70. ESI-HRMS Calculated for $C_{10}H_{11}N_2O$ $[M+H]^+$:175.0871, Found:175.0852.

4.2.8. N-(prop-2-yn-1-yl)-4-(N-(vinylsulfonyl)vinylsulfonamido) benzamide (13)

A stirred solution of 4-amino-*N*-(prop-2-yn-1-yl)benzamide (**12**) (1.0 g, 5.74 mmol) and triethylamine (2.386 mL, 17.22 mmol) in DCM (20 mL) was cooled to 0 °C with ice-bath and 2-chloroethanesμlfonyl chloride (1.86 mL, 17.22 mmol) was then injected slowly. The reaction mixture was stirred at 0 °C for 1 h, and water (100 mL) was added. The product was extracted with DCM (3 × 20 mL). The combined organic extracts were washed with brine (10 mL) and dried over anhydrous Na_2SO_4. The solvent was removed under vacuum and residue was purified by column chromatography on a gradient form petroleum ether to 50% ethyl acetate in petroleum ether to afford 1.51 g (4.25 mmol, 74%) yield of **13** as a yellow solid. ^{1}H NMR (500 MHz, DMSO-d_6) δ 9.08 (t, J = 5.5 Hz, 1H), 7.96–7.88 (m, 2H), 7.51–7.41 (m, 2H), 7.27 (dd, J = 16.3, 9.8 Hz, 2H), 6.40 (dd, J = 9.8, 1.0 Hz, 2H), 6.27 (dd, J = 16.3, 1.0 Hz, 2H), 4.07 (dd, J = 5.5, 2.5 Hz, 2H), 3.14 (t, J = 2.5 Hz, 1H). ^{13}C NMR (126 MHz, DMSO-d_6) δ 165.51, 136.54, 136.31, 136.02, 132.01, 131.53, 129.00, 81.50, 73.50, 29.09. ESI-HRMS Calculated for $C_{14}H_{15}N_2O_5S_2$ $[M+H]^+$:355.0422 Found:355.0451.

4.2.9. N_3-PEG$_3$-MMAE (14)

Monomethyl auristatin E (100.0 mg, 0.14 mmol), 2-(2-(2-(2-azidoethoxy)ethoxy)ethoxy)acetic acid (34.9 mg, 0.15 mmol), HOAt (37.9 mg, 0.28 mmol), EDCl (53.5 mg, 0.28 mmol) and N'N-diisopropylethylamine (140.6 mg, 1.39 mmol) were dissolved in DMF (5 mL). The reaction mixture was stirred at room temperature overnight. The resulting crude mixture was purified by HPLC (10–100% MeCN/H_2O over 30 min) to afford 111 mg (0.12 mmol, 85%) yield of **14** as a white solid. ESI-HRMS Calculated for $C_{47}H_{81}N_8O_{11}$ $[M+H]^+$:993.6025, Found:993.6059.

4.2.10. 6-PEG$_3$-MMAE(15)

N_3-PEG$_3$-MMAE (**14**) (37 mg, 0.0397 mmol), **6** (15.58 mg, 0.0476 mmol), Na ascorbate (8.38 mg, 0.0476 mmol) and $CuSO_4$ (7.57 mg, 0.0476 mmol) were dissolved in ^{t}BuOH/H_2O/DMF (1/1/1) (6 mL). The reaction mixture was stirred at room temperature for 2 h. Upon completion, the resulting crude mixture was purified by HPLC (10–100% CH_3CN/H_2O over 30 min) to afford 14.6 mg (0.01158 mmol, 29%) yield of **15** as a white solid. ESI-HRMS Calculated for $C_{60}H_{94}N_9O_{16}S_2$ $[M+H]^+$:1260.6260, Found:1260.6296. The product was analyzed by HPLC for purity of 98%. ^{1}H NMR (500 MHz, CD_3OD) δ 8.21–8.14 (m, 1H), 7.99–7.94 (m, 1H), 7.41–7.35 (m, 2H), 7.35–7.27 (m, 2H), 7.24–7.19 (m, 3H), 7.15–7.05 (m, 4H), 6.23 (ddd, J = 11.7, 3.9, 2.0 Hz, 4H), 5.21 (s, 2H), 4.81–4.47 (m, 5H), 4.46–4.00 (m, 4H), 4.00–3.79 (m, 3H), 3.75–3.52 (m, 9H), 3.45–3.33 (m, 6H), 3.30–3.25 (m, 3H), 3.11 (d, J = 3.2 Hz, 1H), 3.02–2.89 (m, 4H), 2.56–2.42 (m, 2H), 2.38–1.21 (m, 10*H*), 1.21–1.10 (m, 6H), 1.06–0.79 (m, 19H). ^{13}C NMR (126 MHz, CD_3OD) δ 175.71, 175.42, 172.71, 171.89, 171.75, 171.56, 161.13, 144.31, 144.09, 143.89, 137.65, 133.60, 130.59, 129.53, 129.23, 128.62, 128.38, 128.18, 128.08, 127.89, 126.44, 126.33, 116.48, 86.70, 83.51, 77.54, 77.25, 71.73, 71.55, 71.51, 71.44, 71.42, 70.61, 70.30, 63.68, 63.57, 62.68, 61.99, 61.50, 60.78, 60.59, 58.62, 58.35, 56.31, 56.11, 51.52, 51.43, 50.74, 48.07, 45.88, 45.53, 38.31, 36.94, 33.91, 31.85, 31.64, 30.38, 27.70, 27.61, 26.99, 26.60, 25.84, 25.64, 24.45, 19.76, 19.14, 18.97, 18.79, 18.72, 16.94, 16.31, 15.94, 15.83, 14.99, 10.90.

4.2.11. 10-PEG$_3$-MMAE (16)

N_3-PEG$_3$-MMAE (**14**) (37 mg, 0.0397 mmol), **10** (18.21 mg, 0.0476 mmol), Na ascorbate (8.38 mg, 0.0476 mmol) and $CuSO_4$ (7.57 mg, 0.0476 mmol) were dissolved in ^{t}BuOH/H_2O/DMF (1/1/1) (6 mL). The reaction mixture was stirred at room temperature for 2 h. Upon completion, the resulting crude mixture was purified by HPLC (10–100% MeCN/H_2O over 30 min) to afford 6.1 mg (0.0463 mmol, 11%) yield of **16** as a white solid. ESI-HRMS Calculated for $C_{63}H_{99}N_{10}O_{16}S_2$ $[M + H]^+$:1315.6682, Found:1315.6658. The product was analyzed by HPLC for purity of 98%. ^{1}H NMR (500 MHz, CD_3OD) δ 8.01–7.92 (m, 1H), 7.89–7.81 (m, 1H), 7.65 (dt, J = 8.7, 1.1 Hz, 2H), 7.41–7.35 (m, 2H), 7.36–7.27 (m, 2H), 7.25–7.17 (m, 3H), 7.12 (ddd, J = 16.7, 9.8, 1.2 Hz, 2H), 6.28–6.20 (m, 4H), 4.80–4.47 (m, 5H), 4.47–4.01 (m, 4H), 3.97–3.80 (m, 3H), 3.79–3.50 (m, 9H), 3.46–3.33 (m, 6H), 3.30–3.25 (m, 3H), 3.11 (d, J = 3.9 Hz, 1H), 3.04–2.89 (m, 3H), 2.78 (t, J = 7.5 Hz, 2H), 2.57–2.38 (m, 4H), 2.37–1.21 (m, 11*H*), 1.21–1.09 (m, 6H), 1.06–0.74 (m, 19H). ^{13}C NMR (126 MHz, CD_3OD) δ 175.69, 175.41, 173.99, 172.73, 171.88, 171.73, 171.56, 148.11, 144.08, 143.88, 141.93, 137.63, 132.76, 130.68, 130.29, 129.53, 129.23, 128.62, 128.38, 128.08, 127.89, 124.32, 121.21, 86.67, 83.48, 77.53, 77.25, 71.73, 71.50, 71.42, 70.61, 70.37, 63.65, 61.99, 61.51, 60.77, 60.59, 58.61, 58.35, 57.75, 56.31, 56.11, 51.40, 51.30, 50.73, 48.07, 45.87, 45.52, 38.29, 37.15, 33.62, 33.10, 31.84, 30.36, 27.71, 27.62, 26.98, 26.58, 26.41, 25.84, 25.75, 25.63, 24.45, 19.75, 19.16, 18.98, 18.72, 16.95, 16.31, 15.97, 15.83, 15.00, 10.90.

4.2.12. 13-PEG$_3$-MMAE (17)

N_3-PEG$_3$-MMAE (**14**) (30 mg, 0.032 mmol), **13** (13.82 mg, 0.039 mmol), Na ascorbate (6.87 mg, 0.039 mmol) and $CuSO_4$ (6.2 mg, 0.039 mmol) were dissolved in ^{t}BuOH/H_2O/DMF (1/1/1) (6 mL). The reaction mixture was stirred at room temperature for 2 h. Upon completion, the resulting crude mixture was purified by HPLC (10–100% MeCN/H_2O over 30 min) to afford 17.5 mg (0.0136 mmol, 42%) yield of **17** as a white solid. ESI-HRMS Calculated for $C_{63}H_{99}N_{10}O_{16}S_2$ $[M+H]^+$:1287.6369, Found:1287.6390. The product was analyzed by HPLC for purity of 94%. ^{1}H NMR (500 MHz, CD_3OD) δ 8.03–7.96 (m,

1H), 7.92 (ddd, J = 8.4, 4.3, 1.9 Hz, 3H), 7.43–7.36 (m, 4H), 7.31 (dt, J = 14.0, 7.6 Hz, 2H), 7.24–7.19 (m, 1H), 7.15 (ddd, J = 16.5, 9.8, 1.3 Hz, 2H), 6.30–6.20 (m, 4H), 4.80–4.46 (m, 7H), 4.31–4.13 (m, 3H), 3.90–3.84 (m, 2H), 3.78–3.50 (m, 9H), 3.45–3.33 (m, 6H), 3.30–3.25 (m, 3H), 3.11 (d, J = 4.3 Hz, 1H), 3.02–2.90 (m, 3H), 2.60–1.21 (m, 13H), 1.21–1.10 (m, 6H), 1.07–0.81 (m, 19H). ^{13}C NMR (126 MHz, CD_3OD) δ 175.70, 175.41, 175.07, 172.74, 171.87, 171.74, 171.59, 168.69, 146.14, 144.08, 143.88, 138.23, 137.51, 137.20, 132.43, 131.11, 129.58, 129.54, 129.24, 128.62, 128.39, 128.08, 127.90, 125.24, 86.66, 83.48, 78.87, 77.53, 77.25, 71.83, 71.69, 71.50, 71.40, 71.37, 71.08, 70.53, 70.33, 63.64, 63.54, 61.99, 61.51, 60.77, 60.58, 58.61, 58.35, 56.34, 56.13, 51.42, 48.07, 45.86, 45.52, 38.27, 36.36, 33.62, 31.83, 30.34, 27.73, 27.65, 26.98, 26.58, 25.84, 25.63, 24.46, 19.75, 19.71, 19.36, 19.17, 18.99, 18.74, 16.95, 16.32, 15.97, 15.82, 15.01, 10.90.

4.3. Antibody-drug conjugates

To a solution of Trastuzumab (100 μL, 20 μM, 3 mg/mL) in PBS (137 mM NaCl, 2.67 mM KCl, 10 Mm Na_2HPO_4, 2 mM KH_2PO_4, pH 7.2–7.4) was added tris(2-carboxyethyl)phosphine (TCEP, 10 eq.,2 μL, 10 mM stock solution in H_2O, pH 7.07 was adjusted by NaOH and H_3PO_4). The mixture was vortexed and incubated at 37 °C for 1 h. The solutions of compounds 15–17 (10 mM in DMSO, 20 eq., 4 μL) was added respectively and the reaction mixture incubated at 37 °C for 12 h. The excess reagents were removed by repeated diafiltration into PBS using an Zeba™ Spin Desalting Columns (Thermo, 7K MWCO, 0.5 mL). The resulting conjugates were characterized by MS and SEC analysis.

4.4. Cell lines and culture

Cancer cell lines SK-BR-3, MCF7, MDA-MB-468, HCC827 and NCI-H2228 were obtained from American Type Culture Collection (ATCC, Manassas, VA, USA). Fetal bovine serum (FBS), RPMI 1640 medium, DMEM medium, MEM medium, Penicillin-Streptomycin (PS), non-essential amino acid (NEAA) were purchased from Gibco Thermofisher Scientific (Waltham, MA. USA). Recombinant human insulin was purchased from Sigma Chemical (St. Louis, MO, USA). SK-BR-3 and MDA-MB-468 cells were cultured in DMEM medium with 10% FBS and 1% PS; HCC827 and NCI-H2228 cells were cultured in RPMI 1640 medium with 10% FBS and 1% PS; MCF7 cell was cultured in MEM medium with 10% FBS, 1% PS, 1% NEAA and 10 μg/mL insulin; all cells were cultured at 37 °C in a humidified incubator with 5% CO_2.

4.5. Cytotoxicity assay

Cytotoxicity assay of ADCs **18**–**20** was performed on SK-BR-3, MCF7, MDA-MB-468 and HCC827 and NCI-H2228 cells; ADCs **21**–**23** was performed on HCC827 and NCI-H2228 cells. Briefly, cells (5×10^3 cells/well) were cultured in 96-well plates with 100 μL complete medium, and 24 h later the cells were treated in triplicate with varying concentrations of ADCs, MMAE, T-DM1, herceptin or cetuximab for 72 h. The cells cultured in medium alone served as the control and medium alone served as the blank. Cell viability was determined using Cell Counting Kit-8 (CCK-8) kit according to the manufacturer's instructions. The absorbent optical density (OD) values at 450 nm were measured in a microplate reader (SpectraMax i3, MD, USA). The inhibition rate of cell growth in individual wells was determined using the following formula: growth inhibition rate = (OD value of control − OD value of dose)/(OD value of control − OD value of blank) × 100%. The half maximal inhibitory concentrations (IC_{50}) of the compounds for each cell were calculated using the Prism 7 software.

4.6. Flow cytometry for affinity of ADCs

Goat Anti-Human IgG H&L (FITC) was purchased from Abcam (Cambridge, UK). DAPI was purchased from Cell Signaling Technology (Boston, USA). HCC827 and NCI-H2228 cells (2×10^5 cells/tube) were collected and incubated with varying concentrations of ADCs and cetuximab at 4 °C for 30 min. After being washed with FACE solution (1% BSA in PBS, pH 7.4), the cells were stained with Goat Anti-Human IgG H&L (FITC) (1:200) at 4 °C for 30 min. After being washed with FACE solution, the cells were stained with DAPI (1 μg/mL) in PBS. The fluorescent signals in individual samples were detected by CytoFLEX flow cytometer (Beckman Coulter, Brea, USA) and analyzed using the FlowJo software.

4.7. Flow cytometry for internalization of ADCs

HCC827 cell (2×10^5 cells/tube) was collected and incubated with ADCs and cetuximab in duplicate at 4 °C for 30 min. After being washed with FACE solution, the samples were incubated with PBS at 4 °C and 37 °C for 3 h. And then the samples were incubated with Goat Anti-Human IgG H&L (FITC) (1:200) at 4 °C for 30 min. After being washed with FACE solution, the cells were stained with DAPI (1 μg/mL) in PBS. The fluorescent signals in individual samples were detected by CytoFLEX flow cytometer (Beckman Coulter, Brea, USA) and analyzed using the FlowJo software. The percentage of internalization was determined using the following formula: percentage of internalization = (fluorescence intensity of cells at 4 °C – fluorescence intensity of cells at 37 °C)/fluorescence intensity of cells at 4 °C × 100%.

4.8. In vivo efficacy study

All experimental protocols were approved by Animal Ethics Committee of ShanghaiTech University. All procedures in efficacy study were conducted according to the Animal Welfare Act and Regulations published by the US National Institutes of Health. Five-week-old Nod-Scid male mice were purchased from GemPharmatech Co., Ltd (Nanjing, China). After acclimatization for one week, healthy mice were subcutaneously implanted with 5×10^6 HCC827 cells. Fourteen days after implantation the mice were divided into three groups (n = 8 each): **21**, **22** and PBS as control. All the groups received four doses of 20 mg/kg on days 0, 4, 8 and 12, injected intravenously. Tumor volume and body-weight were measured at regular intervals. Tumor volumes were calculated with the formula: (mm^3) = (length × $width^2$)/2.

The animals were housed (4 mice/cage) in a specific pathogen-free (SPF) animal laboratory of the National Center for Protein Science Shanghai (Shanghai, China) under standard laboratory conditions (adequate fresh air exchange, temperature 20–24 °C and relative humidity 40–70%). A 12-h light/dark automatic cycle of artificial illumination was used. All animals were provided sterile drinking water.

Declaration of Competing Interest

The authors declare that they have no known competing financial interests or personal relationships that could have appeared to influence the work reported in this paper.

Acknowledgements

We thank Cunliang Zhao at Jing Medicine for his help to support this research, Dr. Wei Huang and Dr. Feng Tang at Shanghai Institute of Materia Medica (SIMM), Chinese Academy of Sciences for providing Endo-S. This work was supported by the grant from China Postdoctoral Science Foundation (2019M651608).

Appendix A. Supplementary material

Supplementary data to this article can be found online at https://doi.org/10.1016/j.bmc.2020.115793.

References

1 Beck A, Goetsch L, Dumontet C, Corvaia N. Strategies and challenges for the next generation of antibody-drug conjugates. *Nat Rev Drug Discov*. 2017;16:315–337.
2 Chari RV, Miller ML, Widdison WC. Antibody-drug conjugates: an emerging concept in cancer therapy. *Angew Chem Int Ed Engl*. 2014;53:3796–3827.
3 Lyon R. Drawing lessons from the clinical development of antibody-drug conjugates. *Drug Discov Today Technol*. 2018;30:105–109.
4 Abdollahpour-Alitappeh M, Lotfinia M, Gharibi T, et al. Antibody-drug conjugates (ADCs) for cancer therapy: Strategies, challenges, and successes. *J Cell Physiol*. 2019;234:5628–5642.
5 Rodrigues T, Bernardes GJL. Development of Antibody-Directed Therapies: Quo Vadis? *Angew Chem Int Ed Engl*. 2018;57:2032–2034.
6 Krall N, da Cruz FP, Boutureira O, Bernardes GJ. Site-selective protein-modification chemistry for basic biology and drug development. *Nat Chem*. 2016;8:103–113.
7 Chudasama V, Maruani A, Caddick S. Recent advances in the construction of antibody-drug conjugates. *Nat Chem*. 2016;8:114–119.
8 Forte N, Chudasama V, Baker JR. Homogeneous antibody-drug conjugates via site-selective disulfide bridging. *Drug Discov Today Technol*. 2018;30:11–20.
9 Badescu G, Bryant P, Bird M, et al. Bridging disulfides for stable and defined antibody drug conjugates. *Bioconjug Chem*. 2014;25:1124–1136.
10 Shaunak S, Godwin A, Choi JW, et al. Site-specific PEGylation of native disulfide bonds in therapeutic proteins. *Nat Chem Biol*. 2006;2:312–313.
11 Bryant P, Pabst M, Badescu G, et al. In Vitro and In Vivo Evaluation of Cysteine Rebridged Trastuzumab-MMAE Antibody Drug Conjugates with Defined Drug-to-Antibody Ratios. *Mol Pharm*. 2015;12:1872–1879.
12 Lee MTW, Maruani A, Baker JR, Caddick S, Chudasama V. Next-generation disulfide stapling: reduction and functional re-bridging all in one. *Chem Sci*. 2016;7:799–802.
13 Schumacher FF, Nunes JP, Maruani A, et al. Next generation maleimides enable the controlled assembly of antibody-drug conjugates via native disulfide bond bridging. *Org Biomol Chem*. 2014;12:7261–7269.
14 Smith ME, Schumacher FF, Ryan CP, et al. Protein modification, bioconjugation, and disulfide bridging using bromomaleimides. *J Am Chem Soc*. 2010;132:1960–1965.
15 Assem N, Ferreira DJ, Wolan DW, Dawson PE. Acetone-Linked Peptides: A Convergent Approach for Peptide Macrocyclization and Labeling. *Angew Chem Int Ed Engl*. 2015;54:8665–8668.
16 Ramos-Tomillero I, Perez-Chacon G, Somovilla-Crespo B, et al. Bioconjugation through Mesitylene Thiol Alkylation. *Bioconjug Chem*. 2018;29:1199–1208.
17 Martinez-Saez N, Sun S, Oldrini D, et al. Oxetane Grafts Installed Site-Selectively on Native Disulfides to Enhance Protein Stability and Activity In Vivo. *Angew Chem Int Ed Engl*. 2017;56:14963–14967.
18 Griebenow N, Dilmac AM, Greven S, Brase S. Site-Specific Conjugation of Peptides and Proteins via Rebridging of Disulfide Bonds Using the Thiol-Yne Coupling Reaction. *Bioconjug Chem*. 2016;27:911–917.
19 Walsh SJ, Omarjee S, Galloway W, et al. A general approach for the site-selective modification of native proteins, enabling the generation of stable and functional antibody-drug conjugates. *Chem Sci*. 2019;10:694–700.
20 Zhang Y, Zang C, An G, et al. Cysteine-specific protein multi-functionalization and disulfide bridging using 3-bromo-5-methylene pyrrolones. *Nat Commun*. 2020;11:1015.
21 Li Z, Huang R, Xu H, et al. Divinylsulfonamides as Specific Linkers for Stapling Disulfide Bonds in Peptides. *Org Lett*. 2017;19:4972–4975.
22 Huang R, Sheng Y, Wei D, Yu J, Chen H, Jiang B. Bis(vinylsulfonyl)piperazines as efficient linkers for highly homogeneous antibody-drug conjugates. *Eur J Med Chem*. 2020;190:112080.
23 Hamblett KJ, Senter PD, Chace DF, et al. Effects of drug loading on the antitumor activity of a monoclonal antibody drug conjugate. *Clin Cancer Res*. 2004;10:7063–7070.